HOSTED BY

ELSEVIER

CrossMark

Available online at www.sciencedirect.com

ScienceDirect

Journal of Magnesium and Alloys 2 (2014) 214–219
www.elsevier.com/journals/journal-of-magnesium-and-alloys/2213-9567

Full length article

The effect of strontium on the microstructure and mechanical properties of Mg–6Al–0.3Mn–0.3Ti–1Sn

Hüseyin Şevik [a,b,*], S. Can Kurnaz [a]

[a] *Sakarya University, Faculty of Engineering, Department of Metallurgical and Materials Engineering, Adapazarı 54187, Turkey*
[b] *Mersin University, Faculty of Engineering, Department of Metallurgical and Materials Engineering, Mersin 33343, Turkey*

Received 3 April 2014; revised 17 June 2014; accepted 11 August 2014
Available online 18 October 2014

Abstract

In this work, the microstructural and mechanical properties of the certain magnesium-based alloys were investigated. The alloys were produced under a controlled atmosphere by a squeeze-casting process and characterized by optical microscopy (OM), scanning electron microscopy (SEM), an energy-dispersive spectrometer (EDS) and X-ray diffraction (XRD) analysis. The results indicated that the addition of strontium element modified the structure and refined the grain size. The hardness and yield strength of the alloys increased continuously with increasing strontium content, while the elongation was gradually decreased. Also, the tensile strength value of the based alloy was increased by adding Sr up to 1 wt.%. After more addition of Sr, the tensile strength starts to diminish.

Keywords: Mg–Al alloy; Strontium; Microstructure; Mechanical testing

1. Introduction

To save fuel costs and lower emissions, the transportation industry needs to use lighter and stronger materials. Therefore, magnesium alloys are highly attractive structural materials due to their low density and high specific strength. Magnesium alloys are based on Mg–Al and Mg–Al–Zn alloy systems that are the most common materials used in the automotive industry [1–4]. However, these alloys have limitations in their use because of the lower strength, ductility and corrosion resistance than that aluminium alloys. To increase the areas of usage, there are various alloy designs with alloying elements such as Strontium, Calcium, Silicon, Tin and Rare Earth elements that are examined by researchers [5–15]. Strontium in Mg–Al alloys is one of the most effective alloying elements to improve the strength at room and elevated temperatures [5,7,9,14]. Tin as an alloying element can improve the strength of the magnesium based alloy at room temperature via solid solution hardener [8,10,11]. The effect of Sr addition on the microstructure and mechanical properties of Mg–Al alloys have been investigated by many researchers, as well Sn [12,15]. However, only a few studies [16,17] have examined the effect of Sr and Sn on the microstructure and mechanical properties of Mg–Al alloys. As a result, in this study, Mg–6Al–0.3Mn–0.3Ti–1Sn alloy is selected as the base alloy because of our previous studies [18,19] and Sr element is added to the base alloy, then the effect of Sr on the microstructure and mechanical properties of the base alloy was investigated.

2. Experimental details

The bulk compositions of the alloys studies in the present work are presented in Table 1. The alloys were prepared in an

* Corresponding author. Sakarya University, Faculty of Engineering, Department of Metallurgical and Materials Engineering, Adapazarı 54187, Turkey. Tel.: +90 2642955789; fax: +90 2642955549.
E-mail addresses: sevik@mersin.edu.tr, sevik@sakarya.edu.tr (H. Şevik).
Peer review under responsibility of National Engineering Research Center for Magnesium Alloys of China, Chongqing University.

http://dx.doi.org/10.1016/j.jma.2014.08.001.

Table 1
The chemical composition of the investigated alloys (mass fraction, %).

Alloy no:	Alloy	Al	Mn	Sn	Ti	Sr	Mg
Alloy 1	Mg–6Al–1Sn–0.3Mn–0.3Ti	5.875	0.296	0.924	0.274	–	Bal.
Alloy 2	Mg–6Al–1Sn–0.3Mn–0.3Ti–0.5Sr	5.939	0.251	0.958	0.280	0.483	Bal.
Alloy 3	Mg–6Al–1Sn–0.3Mn–0.3Ti–1Sr	5.992	0.287	0.898	0.239	0.897	Bal.
Alloy 4	Mg–6Al–1Sn–0.3Mn–0.3Ti–2Sr	6.032	0.269	0.978	0.289	1.965	Bal.

electric resistance furnace using a mild steel crucible under a gas mixture of carbon dioxide (CO_2) and sulphur hexafluoride (0.2% SF_6) from commercially pure magnesium, aluminium and tin. Manganese, titanium and Strontium were added in Al–10Mn, Al–6Ti and Mg–20Sr form as a master alloy. The melt was held at 760 °C casting temperature for 30 min, and then poured into mould which was preheated to 270 °C and with 85 MPa filling pressure.

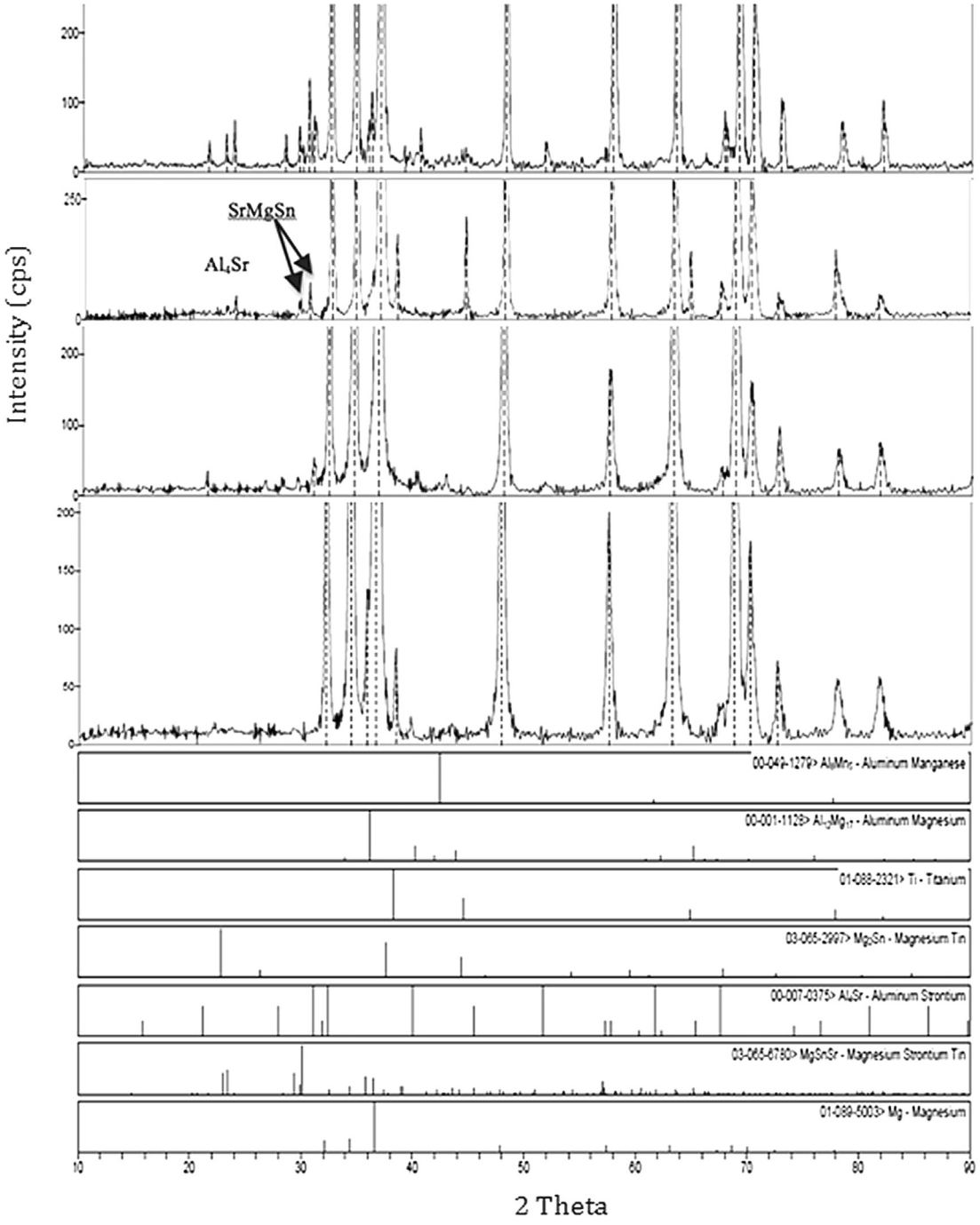

Fig. 1. The X-ray diffraction analysis patterns of the alloys.

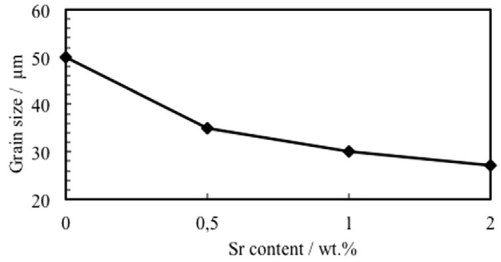

Fig. 2. The effect of Sr on grain size of alloy.

Metallographic samples were prepared based on the standard metallographic procedures. The specimens for optical microscopy were chemically etched in acetic picric (5 ml acetic acid, 6 g picric acid, 10 ml distilled water, 100 ml ethanol). In addition, the distribution of alloying elements in the structure was verified using the scanning electron microscopy (SEM) instrument (JEOL 6060LV) with an energy-dispersive spectrometer (EDS). X-ray diffraction (XRD) analysis was also carried out to identify the phases present in the experimental alloys using a Rigaku D-Max 1000 X-ray diffractometer with CuKα radiation. The grain size measurements were performed using the image analysis software (Clemex).

Brinell hardness testings of the alloys were carried out on ground and polished samples with a ball diameter of 2.5 mm and an applied load of 31.25 kg. At least 10 readings were made to determine the mean value of the hardness at different locations to circumvent the effect of any alloying element segregation. Vickers hardness measurements of metallographically polished specimens were conducted using Leica VHMT MOT microhardness tester with a load of 20 g and holding time of 20 s. Uniaxial tensile tests were performed using an Instron 3367 universal testing machine with a ram velocity of 0.2 mm/min at room temperature (according to ASTM E8M-04). Each test was repeated for ten times, and the average values were accepted as the experimental result.

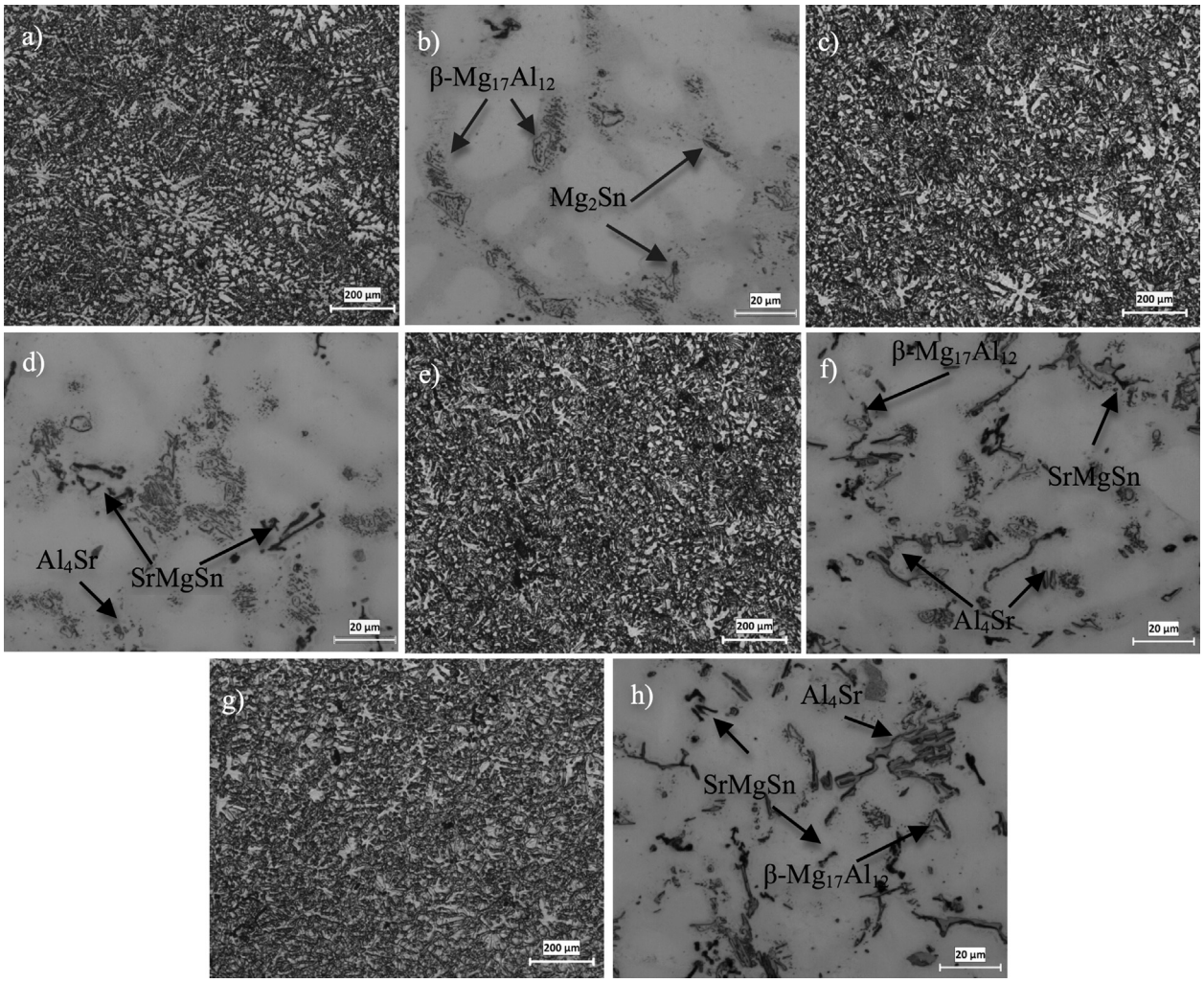

Fig. 3. Optical microscopy microstructures of; (a) and (b) Mg–6Al–0.3Mn–0.3Ti–1Sn, (c) and (d) Mg–6Al–0.3Mn–0.3Ti–1Sn–0.5Sr, (e) and (f) Mg–6Al–0.3Mn–0.3Ti–1Sn–1Sr, (g) and (h) Mg–6Al–0.3Mn–0.3Ti–1Sn–2Sr.

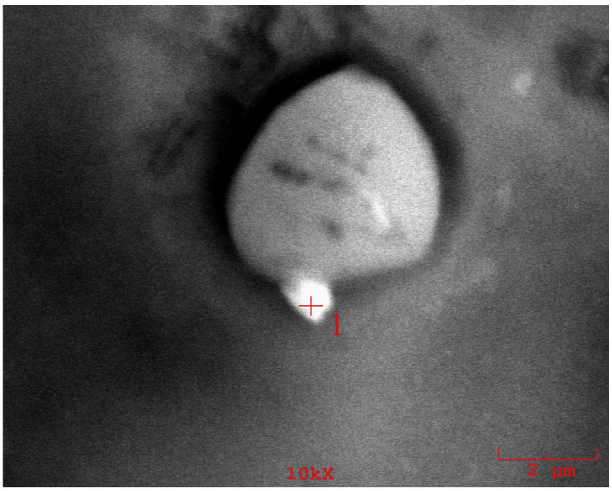

Spot No:	Chemical compositions, (at.%)				
	Al	Mn	Sn	Ti	Mg
1	38.00	-	-	9,76	52,23

Fig. 4. EDS pattern of the Mg–6Al–0.3Mn–0.3Ti–1Sn alloy.

3. Results and discussion

3.1. Microstructure and characterization

Fig. 1 shows the X-ray diffraction patterns. The X-ray results revealed that the Mg–6Al–0.3Mn–0.3Ti–1Sn alloy mainly composed of α-Mg, α-Ti, $Mg_{17}Al_{12}$, Al_8Mn_5 and Mg_2Sn phases. The addition of Sr to base alloy led to the formation of new intermetallic phases-Al_4Sr and SrMgSn. However, the peak of Mg_2Sn was not observed in the modified alloys. The reason is that the addition of Sr to base alloy could be limited the formation of Mg_2Sn intermetallic phase because of existence of SrMgSn intermetallic.

The effect of the Sr addition on the grain size is shown in Fig. 2. This figure shows that the grain size decreased as the Sr increased. In the past, many studies [12,15,20–23] have also showed that the Sr had a significant grain refining effect in Mg–Al alloy system. It is well known that Sr has very low solid solubility in Mg matrix (wt.%0.11). During the solidification, Sr solute atoms are rejected to the front of the solid/liquid interface that restricts grain growth and promotes nucleation in the melt. Also, Al_4Sr and SrMgSn intermetallic particles, which have the higher formation temperature, could act as nucleation sites and therefore finer grains were achieved with addition of Sr.

Fig. 3 shows the optical microstructure of the alloys. As seen in Fig. 3a that the primary α-Mg phase in the base alloy are formed as a dendritic morphology. With increasing Sr, the dendritic arms become smaller, as can be seen in Fig. 3c, e and g Also, the Al_4Sr and SrMgSn intermetallic phases are located and dominated along the grain boundaries instead of $Mg_{17}Al_{12}$ (Fig. 3b, d, f and h). The SEM micrograph and EDS analyse of base alloy are shown in Fig. 4. As mentioned above that (Fig. 1), whole alloys contain α-Ti that this finding is confirmed by EDS analyse of base alloy (Fig. 4.). Fig. 5 presents the SEM micrograph and EDS analyse of alloy containing 2 wt.% Sr. It can be said that from Fig. 5a, the SrMgSn intermetallic phase was formed within the grain, as well as grain boundary. According to atomic ratio of Al to Sr, it can be inferred that the spot 1 and 6 in

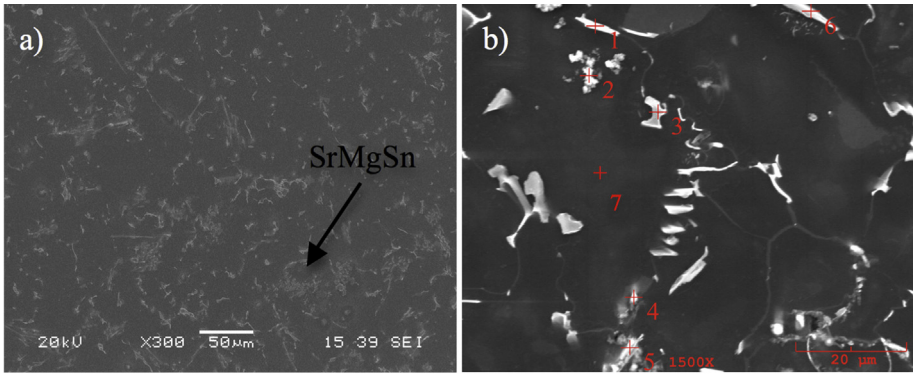

Spot No:	Chemical compositions, (at.%)					Atomic ratio			
	Al	Mn	Sn	Sr	Mg	Sn/Sr	Al/Mn	Al/Sr	Mg/Al
1	38.00	-	-	9,76	52,23	-	-	3,89	1,37
2	25,80	22,96	-	-	51,46	-	1,12	-	1,99
3	34.01	-	-	2,55	63,42	-	-	-	1,86
4	4,08	-	2,07	1,95	91,9	1,06	-	2,09	-
5	8,69	-	5,09	4,69	82,06	1,08	-	1,85	-
6	37,54	-	-	14,03	48,42	-	-	2,67	1,28
7	2,13	-	0,22	-	97,65	-	-	-	-

Fig. 5. SEM and EDS patterns of Mg–6Al–0.3Mn–0.3Ti–1Sn–2Sr alloy.

Table 2
Macro and micro-hardness of the alloys tested.

Alloy no	α-Mg	β-$Mg_{17}Al_{12}$ + Eutectic	Mg_2Sn	Al_4Sr + Eutectic	SrMgSn + Eutectic	SrMgSn + α-Mg	Macro-hardness
1	73 ± 2	206 ± 5	105 ± 6	–	–	–	54 ± 2
2	75 ± 3	–	–	170 ± 1	150 ± 2	–	58 ± 0
3	72 ± 1	–	–	177 ± 3	153 ± 1	–	61 ± 0
4	73 ± 1	–	–	184 ± 6	147 ± 0	136 ± 2	67 ± 1

Table 3
Hardness, yield strength, ultimate tensile strength and elongation of the tested materials.

Alloy no:	Yield strength (MPa)	Ultimate tensile strength (MPa)	ε (%)
Alloy 1	115 ± 4	210 ± 6	8.7 ± 0.2
Alloy 2	130 ± 4	260 ± 8	8.3 ± 0.2
Alloy 3	145 ± 7	262 ± 9	8.1 ± 0.4
Alloy 4	150 ± 5	250 ± 10	7.8 ± 0.2

Fig. 5b were a lamellar intermetallic Al_4Sr phase and the second and third spots can be decided as Al_8Mn_5 and $Mg_{17}Al_{12}$ phases, respectively. Also, the spot 4 and 5 were SrMgSn phase according to atomic ratio of Sr to Sn. Furthermore, the spot 4 was indicated that some Sr solved in the $Mg_{17}Al_{12}$ phase. Besides, it can be seen from spot 7 that the amount of Al solubility in Mg matrix was stable with increasing Sr. When the amount of added Sr to Mg–Al based alloys is more than 2 wt.%, the level of dissolved Aluminium in Mg matrix decreases gradually that deleteriously influences the solid solution strengthening mechanism [14,24]. In this study, the quantity of Al solubility was not changed.

The macro-hardness of the alloys and micro-hardness values of different phases are presented in Table 2. The results indicate that, with addition of Sr, the micro-hardness of the α-Mg remained unchanged, however, with addition of 2 wt.% Sr, the micro-hardness of the grain (mixture phase; α-Mg + SrMgSn) improved because of the existence of SrMgSn intermetallic phase in the grain. Furthermore, the micro-hardness value of Al_4Sr + eutectic and SrMgSn + eutectic mixture phases was found to be 177 Hv and 148 Hv, respectively, which are much higher than the α-Mg, due to the continuous increase in macro-hardness of the alloys.

The tensile properties of base alloy with different strontium additions are presented in Table 3. As can be seen in Table 3 that the yield strength remarkably improved with increasing Sr addition, while the elongation gradually decreased. The maximum yield strength was gained in the alloy containing 2 wt.%Sr. Also, the tensile strength value of the alloy 1 increased by adding Sr up to 1 wt.%. With further addition of Sr, the tensile strength dropped. The enhancement in yield and tensile strength value is attributed to the followings; (1) strengthening by grain refinement, (2) hindering dislocation motion because of Al_4Sr and SrMgSn intermetallic, and finally (3) decreasing detrimental effect of $Mg_{17}Al_{12}$, which is incompatible with magnesium matrix [16,18].

Fig. 6 shows the SEM images of the tensile fracture surface of alloys. Fig. 6a is the image of alloy 1, which indicates mixed-

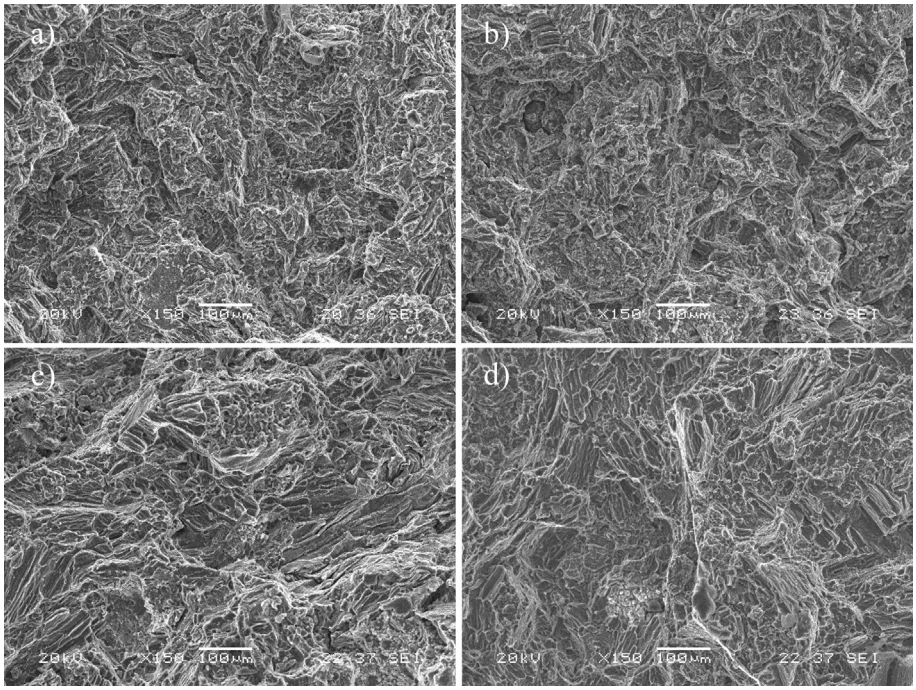

Fig. 6. SEM fractographs showing the morphology of fractured surfaces of (a) Alloy 1, (b) Alloy 2, (c) Alloy 3 and (d) Alloy 4.

mode fracture having features associated with dimple rupture and flat facets. It can be said that amount of the dimple features on the fracture surface of alloy 1 decreased with increasing Sr addition, while increasing the quantity of flat facets. This result can be attributed to the higher amount of second phases.

4. Conclusions

1. The main components were α-Mg α-Ti, $Mg_{17}Al_{12}$, Al_8Mn_5 and Mg_2Sn phases in the base alloy. With addition of Sr, the new intermetallic phases-Al_4Sr and SrMgSn were observed and also, it was shown that the grain size of base alloy could be decreased almost two times from 50 μm to 27 μm.
2. The hardness and yield strength of the alloys continuously increase with increasing strontium concentration, while the elongation was gradually decreased. Also, the tensile strength value of the based alloy was increased by adding Sr up to 1 wt.%. Having added to this critical weight percentage Sr ratio, the tensile strength starts to drop with increasing Sr addition.

Acknowledgements

The authors wish to thank The Scientific and Technical Research Council of Turkey- TUBITAK (grant number: 106M122) for financial support in this study. The authors also would like to thank Mr. Metin GÜNAY for his technical support.

References

[1] N. Hort, Y. Huang, K.U. Kainer, Adv. Eng. Mater. 8 (2006) 235.
[2] L. Zhang, Z.Y. Cao, Y.B. Liu, G.H. Su, L.R. Cheng, Mater. Sci. Eng. A 508 (2009) 129.
[3] M. Pekguleryuz, M. Celikin, Inter. Mater. Rev. 55 (2010) 197.
[4] B. Kim, J. Do, S. Lee, I. Park, Mater. Sci. Eng. A 527 (2010) 6745.
[5] P. Zhao, Q. Wang, C. Zhai, Y. Zhu, Mater. Sci. Eng. A 444 (2007) 318.
[6] S. Li, B. Tang, B.D. Zeng, J. Alloys Compd. 437 (2007) 317.
[7] A. Janz, J. Gröbner, D. Mirkovic, M. Medraj, J. Zhu, Y.A. Chang, R.S. Fetzer, Intermetallics 15 (2007) 506.
[8] C. Jihua, C. Zhenhua, Y. Hongge, Z. Fuquan, L. Kun, J. Alloys Compd. 461 (2008) 209.
[9] Q. Zhang, S.P. Wang, H. Hu, Mater. Technol. 24 (2009) 166.
[10] J. Gröbner, A. Janz, A. Kozlov, D. Mirkovic, R.S. Fetzer, J. Mater. Sci. (December 2008) 32.
[11] H. Liu, Y. Chen, Y. Tang, S. Wei, G. Niu, J. Alloys Compd. 440 (2007) 122.
[12] K. Hirai, H. Soekawa, Y. Takigawa, K. Higashi, Mater. Sci. Eng. A 403 (2005) 276.
[13] M. Masoumi, H. Hu, Mater. Sci. Eng. A 528 (2011) 3589.
[14] E. Baril, P. Labelle, M.O. Pekgüleryüz, J. Mater. (November 2003) 34.
[15] S.F. Liu, B. Li, X.H. Wang, W. Su, H. Han, J. Mater. Process. Technol. 209 (2009) 3999.
[16] B.H. Kim, K.C. Park, Y.H. Park, M. Park, Mater. Sci. Eng. A 528 (2011) 808.
[17] H. Liu, Y. Chen, H. Zhao, S. Wei, W. Gao, J. Alloys Compd. 504 (2010) 345.
[18] H. Sevik, S. Açıkgöz, C. Kurnaz, J. Alloys Compd. 508 (2010) 110.
[19] C. Kurnaz, H. Sevik, S. Açıkgöz, A. Özel, J. Alloys Compd. 509 (2011) 3190.
[20] Y. Lee, A. Dahle, D.H. Stjohn, Metall. Mater. Trans. A 31 (2000) 2895.
[21] P. Yichuan, L. Xiangfa, Y. Hua, J. Wuhan Univ. Technol., Mater. Sci. Ed. 22 (2007) 74.
[22] T.R. Ramachandran, K. Balasubramanian, P. Sharma, in: 68th. World Foundry Congress, February 2008, pp. 189–193.
[23] M. Yang, F. Pan, R. Cheng, A. Tang, Mater. Sci. Eng. 491 (2008) 440.
[24] M. Pekgüleryüz, P. Labelle, D. Argo, E. Baril, Magnesium Technol. (2003) 201–206.